

Multivariate statistical analysis of ^{222}Rn concentration in underground stations of a Chinese city

Y. Shi^{1,2,3}, B. Ding³, J. Zhao⁴, Z. Liu³, L. Wang³, Sh. Wang³, H. Zhao^{1,2,3*}, Y. Liu^{1,2}, G. Wei³, P. Zhang³

¹Harbin Engineering University, College of Physics and Optoelectronic Engineering, Key Laboratory of In-Fiber Integrated Optics of Ministry of Education, Harbin, China

²Harbin Engineering University, Key Laboratory of Photonic Materials and Devices Physics for Oceanic Applications, Ministry of Industry and Information Technology of China, Harbin, China

³Heilongjiang Institute of Atomic Energy, Key Laboratory of Nuclear Technology Application, Harbin, China

⁴Harbin Engineering University, College of Nuclear Science and Technology, Harbin, China

► Original article

*Corresponding author:

Hongtao Zhao, M.D.,

E-mail:

zhaohongtao2019@163.com

Received: February 2024

Final revised: October 2024

Accepted: October 2024

Int. J. Radiat. Res., July 2024; 23(3): 697-705

DOI: 10.61186/ijrr.23.3.26

Keywords: Radon, occupational exposure, radioactivity, multivariate analysis.

INTRODUCTION

Natural sources account for over 98% of radiation exposure in humans, with approximately 52% of this attributed to the inhalation of radon and its decay products in indoor settings, including homes and workplaces⁽¹⁻⁴⁾. Radon is a colorless, odorless, and tasteless radioactive gas produced from the decay of uranium and thorium. Radon and its progeny contribute to over half of the natural radiation exposure in humans, accounting for 2.4 mSv⁽⁵⁾. The major isotopes of radon are ^{219}Rn , ^{220}Rn , and ^{222}Rn , with environmental monitoring focusing primarily on ^{222}Rn . Through decay, these isotopes emit the alpha (α) particle. As α is a heavy charged particle with strong ionization capabilities but relatively weak penetration power, external exposure to α is less harmful to humans but internal exposure through inhalation demands significant attention⁽⁶⁾. When exposed to strong ionizing radiation from α particles, biological tissues and cells in the lungs are ionized and excited, leading to disruptions in their normal metabolism and functions, which can lead to DNA

ABSTRACT

Background: Underground transportation is increasingly becoming the preferred mode of daily commuting. However, radon can accumulate in the relatively enclosed underground environments of subway stations, posing ionizing radiation exposure risk for staff and the public. Therefore, monitoring and assessment are essential.

Materials and Methods: An FD216 environmental radon measurement device was used to monitor the air radon concentrations in 66 underground stations in a Chinese city, including ticket offices, security checkpoints, and platforms. The personal exposure dose was estimated and potential health effects were evaluated. Multivariate statistical analysis was conducted and frequency distribution, Pearson correlation analysis, box plots, and cluster analysis were used to assess the distribution patterns and relationships among radiological parameters.

Results: The ^{222}Rn concentrations ranged from 20.1 to 78.4 Bq/m³, with an average of 51.5 Bq/m³, which is below the Chinese standard limit. The annual effective dose and excess lifetime cancer risk for underground station staff due to inhalation of indoor radon were 0.48 mSv and 1.69×10^{-3} , respectively, compared to 0.12 mSv and 0.42×10^{-3} for the public, which are below the limits established by the International Commission on Radiological Protection. Radon levels within underground stations do not pose a threat to the health of people.

damage and cancer⁽⁷⁾. The International Agency for Research on Cancer identified radon and its progeny to be among the most important carcinogens. Of lung cancer cases, 3% to 14% are attributable to radon, depending on the average radon concentration and methodology^(8,9). According to data from the United States Environmental Protection Agency and National Cancer Institute, radon is responsible for approximately 21,000 cancer-related deaths each year in the United States, representing 10–15% of the total^(10,11). Consequently, radon in the environment has been officially recognized by the World Health Organization (WHO) as one of the top ten health hazards of the early 21st century^(9,12).

Given that most individuals spend more than 80% of their daytime indoors, public exposure to radon occurs predominantly in enclosed environments^(1,10). Due to the health risks associated with radon exposure, its concentrations have been systematically measured and analyzed as part of comprehensive monitoring programs implemented worldwide^(1,3,13,14). In addition, many countries have developed national radon maps and used them to calculate the

disease burden associated with radon exposure⁽¹⁵⁾.

With the development of the economy and accelerated urbanization, the construction and use of underground facilities, including basements and tunnels, have increased. Radon hazards in underground public facilities, primarily subway systems, have acquired significant attention^(16, 17). Radon can be released from the surroundings of underground structures and accumulate due to ventilation limitations, leading to higher concentrations than in above-ground structures⁽¹⁸⁾. Radon sources in underground structures include the rocks, soil, and groundwater around the structures and the building and decoration materials within the structures⁽¹⁹⁻²¹⁾.

In a city in northeastern China, a recently opened subway system has seen significant increases in passenger traffic. However, little is known about the levels of radon within the subway stations in this city. Given the critical environmental risk factor of radon, this study addresses this issue by conducting the inaugural assessment of indoor radon concentrations in the city's subway system. This study aims to evaluate radon levels, calculate the annual effective doses, and determine excess lifetime cancer risks associated with inhalation for the public and subway staff. This assessment is crucial for safeguarding the health of the public and staff and provides a basis for exploring measures to control and reduce radon radiation levels, including designing effective ventilation and exhaust systems.

Given that uranium and radium, the elements from which radon is generated, are widely present in various types of rocks and soils, this study holds relevance for studies in underground stations located in different geological environments. In addition, the radon concentration in subway stations is related to the geological structure, ventilation system, and human traffic; thus, the study of radon in subway stations can inform research in similar environments, although adjustments are required based on the local geological conditions.

MATERIALS AND METHODS

Study area

This study measured the radon concentrations in 66 underground stations in northeastern China, representing an operational track length of approximately 82.91 km. The architectural structure and interior decoration of the stations feature uniform walls and floors, covered with ceramic tiles. Except for transfer stations, the stations are designed as two-level underground structures with island platforms, with the platform located between the up and down train tracks. The background radon concentration in the outdoor environment is approximately 20 Bq/m³⁽²²⁾.

The stations are situated in the Songnen massif, specifically within the southeastern uplifted region of the Songnen Rift Depression. The predominant tectonic features of the pre-Quaternary basement structures are the northeast and northwest-trending faults, forming the fundamental framework of block faulting. This type of block faulting has experienced inherited vertical uplift and subsidence oscillations since the Quaternary period, exerting a significant influence on the regional geomorphic features and the distribution patterns of Quaternary sediments.

Measurement procedure

²²²Rn activity concentration in the air within underground stations was determined in accordance with "GB/T 18883-2022 Standards for indoor air quality" and "HJ 1212-2021 Measurement methods for determination of radon in environmental air"^(23, 24). A FD216 radon measurement device, developed by the Beijing Institute of Uranium Geology in China, was used for on-site measurements. This apparatus has been calibrated and certified by the China National Institute of Metrology, ensuring that its accuracy adheres to the necessary calibration standards.

The position of monitoring points followed certain principles. They were preferably located in areas where people tend to spend longer duration, away from exhaust vents, and in air ducts with high airflow or vortex generation potential. Stable locations in terms of temperature, humidity, and airflow positioned away from walls, floors, and ceilings were selected. In addition, the monitoring points were discreetly placed where passengers could not easily see or reach them. Each station had monitoring points set up at specific locations, including the ticket office and security checkpoint (for staff evaluation), as well as the boarding and disembarking platforms (for public evaluation). One monitoring point was designated for each location. Each monitoring point was measured once, with a measurement duration of 48 h and sampling every 2 h. The average concentration over the 48 h was considered the detected concentration. Meteorological conditions, including atmospheric pressure, temperature, and humidity, were recorded. The sampling inlet of the instruments was set at a height consistent with a person's breathing zone (approximately 1.5 m).

Determination of annual effective doses of radon

The decay products of radon in the air of underground stations enter the human body through the respiratory tract. According to the formula in GB/T 16146-2015 'Requirements for control of indoor radon and its progeny', the Annual Effective Dose caused by radon exposure in underground stations for the public and staff can be calculated according to equation (1)⁽²⁵⁾:

$$E = C_{Rn} \times (DCF_{Rn} + F \times DCF_{RnD}) \times t \quad (1)$$

where E is the Annual Effective Dose in mSv; C_{Rn} is the radon activity concentration value in Bq/m³; DCF_{Rn} is the dose conversion factor for radon in mSv/(Bq·h·m⁻³); DCF_{RnD} is the dose conversion factor for radon progeny in mSv/(Bq·h·m⁻³); F is the equilibrium factor; and t is the annual exposure time in hours. According to values provided in the United Nations Scientific Committee on the Effects of Atomic Radiation report, $DCF_{Rn} = 0.17 \times 10^{-6}$ mSv/(Bq·h·m⁻³) and $DCF_{RnD} = 9.0 \times 10^{-6}$ mSv/(Bq·h·m⁻³) (25, 26). Referring to typical values for indoor equilibrium factors in China, F is taken as 0.5. The underground operates for 16.5 h per day, with trains running at 8 min intervals and staff working for 8 h per day. For the public, the time spent on the platform per train stop does not exceed 8 min. Considering factors such as transfers and multiple rides, the daily platform time of the public was estimated at 2 h. Thus, for staff and the public, the annual exposure times were $8 \times 250 = 2000$ h and $2 \times 250 = 500$ h, respectively.

Determination of excess lifetime cancer risk for radon

The excess lifetime cancer risk attributable to radon (ELCRRn) was determined based on the estimated annual effective dose values, as represented in equation (2) (27, 28):

$$ELCR_{Rn} = E \times DL \times RF_{Rn} \quad (2)$$

Where; ELCRRn represents the excess lifetime cancer risk for radon. DL denotes the duration of life, set at 70 years. RF refers to the risk factor, which indicates the fatal cancer risk per Sievert. International Commission on Radiological Protection (ICRP) 60 proposed the RF value of 0.05 Sv⁻¹ for the public (29). RF_{Rn} is the risk factor for radon exposure in equilibrium with its progeny. According to ICRP, the value of RF_{Rn} is 0.055 Sv⁻¹ (30). The total excess lifetime cancer risk was calculated by aggregating the excess lifetime cancer risks from both external and internal exposure sources.

Statistical analysis

Statistical analysis of the data was conducted using IBM SPSS version 23, encompassing descriptive statistics, one-sample t-tests, frequency analysis, Pearson's correlation coefficient analysis, and cluster analysis. A p-value of less than 0.05 was deemed statistically significant.

RESULTS

Measurement of radon concentration

Table 1 shows the ²²²Rn concentrations within the

underground stations. The average concentrations ranged from 20.1 to 78.4 Bq/m³, with a total mean of 51.5 Bq/m³. The lowest average concentration of ²²²Rn was 20.1 Bq/m³, observed at station 46, while the highest was 78.4 Bq/m³, observed at station 49. The average concentrations of ²²²Rn at ticket offices varied from 20.8 to 75.0 Bq/m³, with a mean of 49.2 Bq/m³. The lowest average concentration was 20.8 Bq/m³ (station 46) and the highest was 75.0 Bq/m³ (station 11). At security checkpoints, the average concentrations of ²²²Rn ranged from 14.3 to 83.2 Bq/m³, with a mean of 48.6 Bq/m³. The lowest average concentration was 14.3 Bq/m³ (station 42) and the highest was 83.2 Bq/m³ (station 49). For platform areas, the average concentrations of ²²²Rn were from 21.4 to 85.5 Bq/m³, with a mean of 56.8 Bq/m³. The lowest average concentration was 21.4 Bq/m³ (station 46) and the highest was 85.5 Bq/m³ (station 50). The concentrations in all underground stations were below the limit of 400 Bq/m³ specified in the "GBZ 116-2002 Control Standards for Radon and Its Progeny in Underground Spaces," as well as the reference level of 100 Bq/m³ set by the "WHO Handbook on Indoor Radon: A Public Health Perspective" (9, 31). In addition, the concentrations were lower than the radon concentration limits established in other countries, such as 200 Bq/m³ in Australia, 800 Bq/m³ for Canada, 250 Bq/m³ for Germany, 200 Bq/m³ for the United Kingdom, and 150 Bq/m³ for the United States (32). A one-sample t-test of the ²²²Rn activity concentrations of the 66 subway stations yielded a p-value of less than 0.05, indicating a statistically significant difference from the 400 Bq/m³ limit. Similarly, one-sample t-tests of the ²²²Rn activity concentrations at the ticket office, security checkpoint, and platform locations of the 66 subway stations resulted in p-values of less than 0.05, revealing statistically significant differences from the 400 Bq/m³ limit.

Health impact assessment

The excess lifetime cancer risk and annual effective dose due to radon within the underground stations are presented in Table 2. E_s and E_p represent the annual effective dose for staff and the public, respectively, while $ELCR_s$ and $ELCR_p$ represent the excess lifetime cancer risk for staff and the public, respectively. For underground station staff, the annual effective dose and excess lifetime cancer risk due to inhaling radon in the station environment were 0.48 mSv and 1.69×10^{-3} , respectively. For the public using the underground, the annual effective dose and excess lifetime cancer risk due to inhaling radon in the station environment were 0.12 mSv and 0.42×10^{-3} , respectively.

Table 1. ^{222}Rn concentration within underground stations.

Station	^{222}Rn activity concentration (Bq/m ³)				Standard Deviation	P-value
	Ticket office	Security checkpoint	Platform	Mean		
1	51.0	50.6	61.8	54.5	5.2	0.000*
2	64.9	66.8	68.9	66.9	1.6	0.000*
3	41.7	50.2	55.7	49.2	5.8	0.000*
4	68.7	72.2	79.3	73.4	4.4	0.000*
5	61.6	51.8	70.3	61.2	7.6	0.000*
6	64.0	59.8	73.3	65.7	5.6	0.000*
7	35.9	31.9	44.9	37.6	5.4	0.000*
8	35.8	45.1	45.6	42.2	4.5	0.000*
9	24.5	28.8	38.8	30.7	6.0	0.000*
10	42.4	39.1	56.2	45.9	7.4	0.000*
11	75.0	76.1	81.4	77.5	2.8	0.000*
12	21.6	20.9	27.0	23.2	2.7	0.000*
13	28.9	22.6	41.9	31.1	8.0	0.000*
14	48.1	57.7	57.0	54.3	4.4	0.000*
15	30.4	37.7	36.8	35.0	3.3	0.000*
16	71.2	61.8	72.0	68.3	4.6	0.000*
17	51.7	55.1	58.4	55.1	2.7	0.000*
18	51.1	53.6	64.9	56.5	6.0	0.000*
19	64.8	59.3	74.3	66.1	6.2	0.000*
20	74.8	75.8	75.1	75.2	0.4	0.000*
21	52.4	50.0	57.7	53.4	3.2	0.000*
22	39.7	46.6	42.8	43.0	2.8	0.000*
23	54.0	53.3	55.3	54.2	0.8	0.000*
24	65.5	55.5	68.7	63.2	5.6	0.000*
25	59.7	68.7	71.8	66.7	5.1	0.000*
26	40.1	35.9	48.0	41.3	5.0	0.000*
27	36.3	40.4	37.5	38.1	1.7	0.000*
28	38.0	43.9	42.2	41.4	2.5	0.000*
29	34.1	26.8	47.9	36.3	8.7	0.000*
30	49.4	41.2	57.8	49.5	6.8	0.000*
31	53.6	49.5	53.9	52.3	2.0	0.000*
32	35.0	32.0	42.2	36.4	4.3	0.000*
33	57.7	56.2	69.2	61.0	5.8	0.000*
34	61.3	58.0	66.9	62.1	3.7	0.000*
35	65.0	58.7	66.8	63.5	3.5	0.000*
36	43.2	53.0	51.4	49.2	4.3	0.000*
37	56.8	63.0	67.8	62.5	4.5	0.000*
38	46.2	49.3	58.5	51.3	5.2	0.000*
39	28.0	28.6	29.2	28.6	0.5	0.000*
40	47.1	46.8	57.7	50.5	5.1	0.000*
41	52.8	53.2	63.1	56.4	4.8	0.000*
42	22.4	14.3	25.2	20.6	4.6	0.000*
43	70.3	72.9	80.2	74.5	4.2	0.000*
44	56.2	57.2	70.8	61.4	6.7	0.000*
45	43.9	38.7	43.9	42.2	2.5	0.000*
46	20.8	18.1	21.4	20.1	1.4	0.000*
47	49.0	44.8	52.8	48.9	3.3	0.000*
48	57.0	53.5	60.1	56.9	2.7	0.000*
49	74.3	83.2	77.7	78.4	3.7	0.000*
50	71.9	77.2	85.5	78.2	5.6	0.000*
51	41.4	33.9	52.2	42.5	7.5	0.000*
52	54.3	45.4	63.3	54.3	7.3	0.000*
53	37.9	30.5	39.3	35.9	3.9	0.000*
54	33.3	26.6	45.4	35.1	7.8	0.000*
55	60.4	55.3	74.8	63.5	8.3	0.000*
56	71.4	64.6	77.8	71.3	5.4	0.000*
57	34.2	33.2	34.8	34.1	0.7	0.000*
58	26.3	34.3	33.5	31.4	3.6	0.000*
59	53.7	49.5	60.1	54.4	4.4	0.000*
60	59.3	56.8	72.1	62.7	6.7	0.000*
61	34.3	36.2	45.8	38.8	5.0	0.000*
62	53.0	58.9	58.3	56.7	2.7	0.000*
63	29.3	32.2	37.7	33.1	3.5	0.000*
64	40.2	36.0	50.0	42.1	5.9	0.000*
65	69.7	61.8	75.3	68.9	5.5	0.000*
66	57.9	67.4	71.8	65.7	5.8	0.000*
Mean	49.2	48.6	56.8	51.5	3.7	0.000*
Standard deviation	14.8	15.4	15.4	14.9	/	/
P-value	0.000*	0.000*	0.000*	0.000*	/	/

*P<0.05

Table 2. Annual effective dose and excess lifetime cancer risk for subway station staff and the public (Es, Ep, ELCRs, ELCRp).

Station	Es (mSv)	Ep (mSv)	ELCRs (10^{-3})	ELCRp (10^{-3})
1	0.51	0.13	1.78	0.45
2	0.62	0.16	2.19	0.55
3	0.46	0.11	1.61	0.40
4	0.69	0.17	2.40	0.60
5	0.57	0.14	2.00	0.50
6	0.61	0.15	2.15	0.54
7	0.35	0.09	1.23	0.31
8	0.39	0.10	1.38	0.34
9	0.29	0.07	1.00	0.25
10	0.43	0.11	1.50	0.38
11	0.72	0.18	2.53	0.63
12	0.22	0.05	0.76	0.19
13	0.29	0.07	1.02	0.25
14	0.51	0.13	1.77	0.44
15	0.33	0.08	1.14	0.29
16	0.64	0.16	2.23	0.56
17	0.51	0.13	1.80	0.45
18	0.53	0.13	1.85	0.46
19	0.62	0.15	2.16	0.54
20	0.70	0.18	2.46	0.61
21	0.50	0.12	1.74	0.44
22	0.40	0.10	1.41	0.35
23	0.51	0.13	1.77	0.44
24	0.59	0.15	2.07	0.52
25	0.62	0.16	2.18	0.55
26	0.39	0.10	1.35	0.34
27	0.36	0.09	1.24	0.31
28	0.39	0.10	1.35	0.34
29	0.34	0.08	1.19	0.30
30	0.46	0.12	1.62	0.40
31	0.49	0.12	1.71	0.43
32	0.34	0.08	1.19	0.30
33	0.57	0.14	2.00	0.50
34	0.58	0.14	2.03	0.51
35	0.59	0.15	2.08	0.52
36	0.46	0.11	1.61	0.40
37	0.58	0.15	2.04	0.51
38	0.48	0.12	1.68	0.42
39	0.27	0.07	0.93	0.23
40	0.47	0.12	1.65	0.41
41	0.53	0.13	1.84	0.46
42	0.19	0.05	0.67	0.17
43	0.70	0.17	2.43	0.61
44	0.57	0.14	2.01	0.50
45	0.39	0.10	1.38	0.34
46	0.19	0.05	0.66	0.16
47	0.46	0.11	1.60	0.40
48	0.53	0.13	1.86	0.46
49	0.73	0.18	2.56	0.64
50	0.73	0.18	2.56	0.64
51	0.40	0.10	1.39	0.35
52	0.51	0.13	1.78	0.44
53	0.34	0.08	1.17	0.29
54	0.33	0.08	1.15	0.29
55	0.59	0.15	2.08	0.52
56	0.67	0.17	2.33	0.58
57	0.32	0.08	1.11	0.28
58	0.29	0.07	1.03	0.26
59	0.51	0.13	1.78	0.44
60	0.59	0.15	2.05	0.51
61	0.36	0.09	1.27	0.32
62	0.53	0.13	1.85	0.46
63	0.31	0.08	1.08	0.27
64	0.39	0.10	1.38	0.34
65	0.64	0.16	2.25	0.56
66	0.61	0.15	2.15	0.54
Mean	0.48	0.12	1.69	0.42
Standard deviation	0.14	0.03	0.49	0.12
P-value	0.000*	0.000*	0.000*	0.000*

* P<0.05

Data analysis

The radon measurement results were statistically analyzed to obtain the most accurate conclusions regarding the radon concentration in underground stations in the Chinese city. The frequency distribution and Quantile-Quantile (Q-Q) plots for the ^{222}Rn results within underground station ticket offices, security checkpoints, and platforms were determined. The corresponding histograms are presented in figures 1 - 3. Measures of central tendency and variability in the dataset were characterized by the arithmetic mean and standard deviation of ^{222}Rn activity concentrations in the underground stations. The skewness of ^{222}Rn in underground station ticket offices, security checkpoints, and platforms was close to zero, indicating that their distributions were approximately symmetrical around the mean. Kurtosis functions as a metric for assessing the prominence of a probability distribution associated with a real-valued random variable. By referencing a standard distribution, kurtosis defines the extent of peakedness or flatness in the distribution. A positive kurtosis value suggests a distribution with a relatively sharp peak, whereas a negative kurtosis value indicates a flatter distribution. In this study, the kurtosis values for the ticket offices, security checkpoints, and platforms were all negative, reflecting flat distributions⁽³³⁾.

Frequency distribution plots display the distribution of a dataset using bar charts, representing the frequency of different data points. In these plots, the class intervals are shown on the horizontal axis, while the frequency counts are plotted on the vertical axis, forming rectangles. The area of each rectangle corresponds to the frequency of the data within that interval. Q-Q plots map the values of corresponding quantiles from two probability distributions onto the x- and y-axes. If the two distributions are similar, the points on the plot will approximately lie along the line $y=x$. If the distributions are linearly related, the points will generally form a straight line, though not necessarily along the line $y=x$. If the sample data follows a normal distribution closely, the points will align along a straight line, where the slope of the line represents the standard deviation and the intercept represents the mean. The activity concentration distribution of ^{222}Rn in ticket offices, security checkpoints, and platforms followed a normal distribution, exhibiting a bell-shaped curve characteristic of normal distribution, which can be a valuable insight for further analysis and modeling. The Q-Q plots in figures 1 to 3 show that the points are situated close to the 45° reference line, suggesting that it is reasonable to assume the distributions are normal.

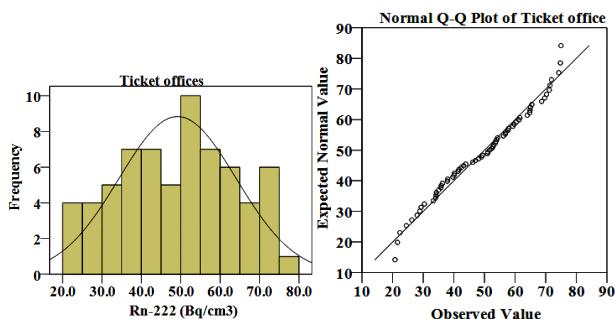


Figure 1. Frequency distribution and quantile-quantile (Q-Q) plots of activity concentrations of ^{222}Rn of ticket offices.

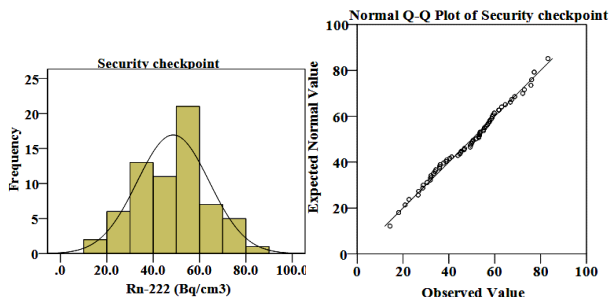


Figure 2. Frequency distribution and quantile-quantile (Q-Q) plots of activity concentrations of ^{222}Rn of security checkpoints.

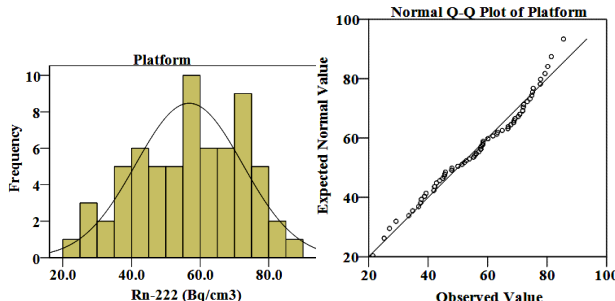


Figure 3. Frequency distribution and quantile-quantile (Q-Q) plots of activity concentrations of ^{222}R of platforms.

Figure 4 displays the distribution of ^{222}Rn activity concentrations within underground station ticket offices, security checkpoints, and platforms. Box plots display the median, which reflects the central tendency of the data. If the median is located in the center of the box, the data distribution is symmetric; if it is not centered, the data is skewed. The length of the box indicates the variability of the data, with longer boxes signifying greater dispersion. The whiskers extending from the box represent the maximum and minimum values within the normal range, while any data points outside this range are considered outliers. If the box and whiskers are of equal length, the data distribution is symmetric; if the lengths of the whiskers vary or if the box is skewed, the data distribution is asymmetrical. The median values were located near the centers of the boxes representing ticket offices, security checkpoints, and platforms, indicating a symmetrical and normally distributed data set⁽³⁴⁾.

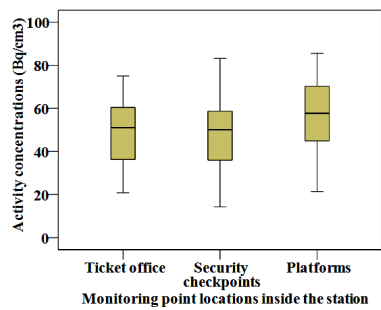


Figure 4. Box plots for the ^{222}Rn results within underground station ticket offices, security checkpoints, and platforms.

The results of the cluster analysis performed to examine the similarities among radiological parameters are shown in figure 5. A dendrogram is a type of chart that displays the hierarchical relationships among objects, groups, or variables. It consists of branches connected at nodes or clusters, which represent groups of observations with similar characteristics. The height of the branches or the distance between the nodes represents the extent of difference or similarity among the groups. In other words, longer branches or increased distances between nodes suggest greater dissimilarity, while shorter branches or reduced distances indicate a higher degree of similarity among the groups. A dendrogram provides a visual representation of clusters with common characteristics. In this study, the average linkage method was employed to quantify the distance between clusters. This method is based on the minimum average distance between clusters, similar to the single and complete linkage techniques. Within the dendrogram, all seven radiological parameters were grouped into two clusters, with Cluster 2 consisting of the following parameters (ticket office, security checkpoint, platform), which exhibited a high degree of similarity. This indicates that the variations in ^{222}Rn concentration within the same underground station in the ticket office, security checkpoint, and platform are correlated.

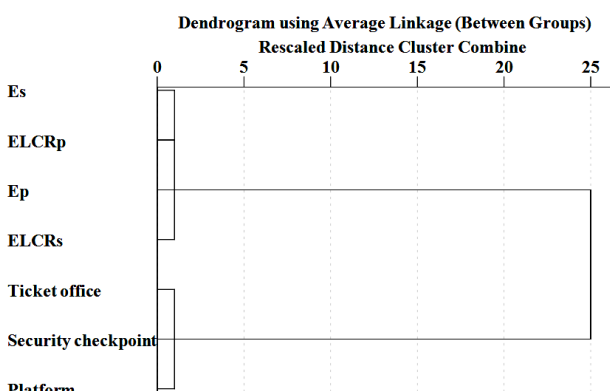


Figure 5. Dendrogram shows the clustering of radiological parameters.

DISCUSSION

Monitoring data from various underground systems in and outside of China are presented in table 3 (19, 21, 35-44). Radon in underground stations primarily originates from building materials, soil, and bedrock emissions. However, the sources and concentrations of radon vary significantly across different regions and stations. In the Kolkata Metro, India, the radon concentration is 23.1 Bq/m³, primarily stemming from emissions in building materials rather than underground soil (19). Older stations with inadequate sealing allow radon to diffuse from bedrock to platforms, resulting in higher radon levels (45). In the Caracas Metro, Venezuela, the radon concentration is 30 Bq/m³ but can reach up to 112 Bq/m³ at fault lines. When underground station and tunnel walls are decorated with granite or marble, a portion of radon can be released into the underground environment (42). The radon concentrations within underground stations in the present study fell within the range observed in other underground systems.

Table 3. ²²²Rn concentration in underground stations in various cities worldwide.

City	Range (Bq/m ³)	Average (Bq/m ³)	References
Guangzhou	9.2-257.5	38.9	(35)
Wuhan	4.7-27.9	13.4	(36)
Nanjing	3.3-45.8	13.5	(37)
Chengdu	12.4-29.0	16.6	(38)
Shenzhen	1.7-95.3	18.3	(39)
Nanning	8.9-35.9	18.5	(40)
Hong Kong	29.6-63.5	41.6	(41)
Xi'an	3.7-166.5	60.7	(42)
Kolkata	13.5-39.0	23.1	(19)
Caracas	/	30.0	(43)
Seoul	7.4-92.5	35.7	(44)
Istanbul	39.47-382.02	114.60	(21)
Chinese city	20.1-78.4	51.5	Present work

The urban subway tunnel is a relatively closed system, where the primary source of radon in the environment comes from the foundation and construction materials. Among these, underground soil and rock formations are the main sources of radon. Radon, released from the several kilometers of rock in the Earth's crust, moves upward through diffusion, permeation, and suction. If the ventilation in underground projects is poor and air circulation is limited, radon can accumulate indoors, reaching very high concentrations. A significant correlation has been found between the radon levels inside buildings and the geological composition of the surrounding area (45-47). Compared to underground station platforms located in non-granite areas, there is a significantly higher possibility of high radon concentrations in underground station platforms situated in granite regions (48). Factors affecting radon concentration also include high temperatures in arid regions, where the warm air at the surface vertically mixes with the air in the underground spaces. This

allows radon to dissipate from underground to outdoor spaces, resulting in lower radon concentrations within underground areas during the summer (49). However, high humidity corresponds to elevated radon concentrations (50, 51). These findings indicate that relative humidity is one of the factors contributing to the increase in radon concentrations.

With the rapid development of underground rail transit in recent years, passenger flow in rail transit has also increased dramatically. An increasing number of personnel (subway staff) are entering underground facilities for work, while more and more passengers rely on underground rail transit for shopping and entertainment. This high volume of passengers' places immense pressure on subway operations and exposes both the public who depend on the subway for travel and the staff to higher radiation risks. Therefore, detecting and evaluating the dose levels of natural radiation exposure (primarily radon and γ radiation) in subway stations is a crucial issue concerning the health and safety of subway staff and millions of passengers. This assessment can provide foundational reference data for researching measures to control and reduce radiation levels. The annual effective doses for staff and the public were below the limits specified in "GB 18871-2002 Basic standards for protection against ionizing radiation and for the safety of radiation sources", at 20 and 1 mSv, respectively (52). Additionally, they were below the recommended limit of 1 mSv/y for public exposure as advised by the ICRP (29). One-sample t-tests of the annual effective doses for employees at the 66 subway stations resulted in a p-value of less than 0.05, indicating a statistically significant difference from the 20 mSv limit. One-sample t-tests of the annual effective doses for the public at the 66 subway stations yielded a p-value of less than 0.05, indicating a statistically significant difference from the 1 mSv limit.

CONCLUSION

The concentrations of ²²²Rn in the subway stations were well below the Chinese standard limit of 400 Bq/m³. For the public, the annual effective dose and excess lifetime cancer risk due to inhaling radon in the station environment were 0.12 mSv and 0.42×10^{-3} , respectively. These values are not harmful to the health of staff or the public. From a multivariate statistical analysis perspective, the activity concentration distribution of ²²²Rn within ticket offices, security checkpoints, and platforms followed a normal distribution. Although the levels complied with international regulatory standards, we recommend undertaking a more extensive survey of natural radiation measurements and the dispersion of indoor radon in all subway stations across the country.

ACKNOWLEDGMENTS

We would like to thank the Scientific Research Business Fee Project of Heilongjiang Provincial Scientific Research Institutes (CZKYF2021-2-B003 and CZJBKYF2023-01), the Ecological Environment Protection Scientific Research Project in Heilongjiang Province (HST2022H001), and the Youth Innovation Fund Project of Heilongjiang Academy of Sciences (CXMS2023YZNY01 and CXMS2023YZNY02) for their support of this research.

Ethical consideration: The authors declare that they have no acknowledged competing financial interests or personal relationships that may have influenced the work presented in this paper.

Funding: This work was supported by the Scientific Research Business Fee Project of Heilongjiang Provincial Scientific Research Institutes (CZKYF2021-2-B003 and CZJBKYF2023-01), Ecological Environment Protection Scientific Research Project in Heilongjiang Province (HST2022H001), Youth Innovation Fund Project of Heilongjiang Academy of Sciences (CXMS2023YZNY01 and CXMS2023YZNY02).

Author contribution: Y.S.: Conceptualization, investigation, data curation, formal analysis and writing - original draft. B.D.: Investigation, formal analysis and writing - review & editing. J.Z.: Formal analysis and writing - review & editing. Z.L.: Writing - review & editing. L.W.: Formal analysis and writing - review & editing. S.W.: Writing - review & editing. H.Z.: Conceptualization, supervision and project administration. Y.L.: Supervision, project administration and project administration. G.W.: Validation and investigation. P.Z.: Validation, investigation and supervision.

REFERENCES

1. Hassanvand H, Birjandi M, Amiri A, Hassanvand MS, Kamarehie B (2019) Investigation of indoor radon concentration in dwellings of Aleshtar (western part of Iran) and estimation of the annual effective dose from exposure to radon. *Int J Radiat Res.*, **17(4)**: 659-666.
2. Ghorbanipour M, Hosseini Alhashemi A, Gharloghi S, Adeli M, Gholami M (2017) Health risk assessment of natural background radiation in residents of Khorramabad, Iran. *Iran J Med Phys.*, **14(1)**: 23-28.
3. Yassin S, Al Sersawi M, Abuzerr S, Darwish M (2019) Indoor radon levels in the dwellings of the Gaza governorate neighborhoods', Palestine. *Int J Radiat Res.*, **17(4)**: 541-548.
4. Shahbazi-Gahrouei D, Setayandeh S, Gholami M (2013) A review on comparison of natural radiation in Iran with other countries. *Int J Low Radiat.*, **9(1)**: 1-11.
5. Nuhu H, Hashim S, Sanusi MSM, Saleh MAM (2022) Radiological assessment subjected to outdoor radon and thoron concentrations and terrestrial gamma radiation measurements in Perak Malaysia. *Appl Radiat Isotopes.*, **179**: 109991.
6. Brooks AL, Khan MA, Duncan A, Buschbom RL, Jostes RF, Cross FT (1994) Effectiveness of radon relative to acute ^{60}Co gamma-rays for induction of micronuclei in vitro and in vivo. *Int J Radiat Biol.*, **66 (6)**: 801-808.
7. Kim ST and Yoo J (2020) Rational establishment of radon exposure standards for dwellings and workplaces. *Int J Radiat Res.*, **18(2)**: 359 -368.
8. Madureira J, Paciência I, Rufo J, Moreira A, de Oliveira Fernandes E, Pereira A (2016) Radon in indoor air of primary schools: determinants factors, their variability and effective dose. *Environ Geochem Health.*, **38(2)**: 523-533.
9. WHO (2009) Handbook on Indoor Radon: A Public Health Perspective, WHO, Geneva.
10. Yeboah SM (2014) Indoor radon in selected homes in Aburi municipality: Measurement uncertainty, decision analysis and remediation strategy: University of Ghana.
11. Mehdipour LA, Saion EB, Sidek A, Halimah M, GoodarzNaseri M, AbdolHalimShaari MN (2013) Influence of chimney effect on the radon effective dose of the lung simulated for radon prone areas of Ramsar in winter season. *IOSR J Appl Phys.*, **4(4)**: 33-7.
12. ICRP (1993) Protection against radon-222 at home and at work, ICRP Publication 65. Ann. ICRP **23(2)**.
13. Oni E A, Oladapo OO, Aremu AA (2022) Preliminary probe of radon content in drinking water in Ibadan, south-western Nigeria. *Int J Radiat Res.*, **20(4)**: 871-877.
14. Alhamdi WA and Abdullah KMS (2022) Estimation of indoor radon concentration and dose evaluation of radon and its progeny in selected dwellings in Duhok city, Kurdistan Region, Iraq. *Int J Radiat Res.*, **20(2)**: 461-466.
15. Pirsahab M, Najafi F, Khosravi T, Hemati L (2013) A systematic review of radon investigations related to public exposure in Iran. *Iran Red Crescent Me.*, **15(11)**: e10204.
16. Doi M and Kobayashi S (1996) Surveys of concentration of radon isotopes in indoor and outdoor air in Japan. *Environ Int.*, **22**: 649-655.
17. Yoon S, Chang BU, Kim Y, Byun JI, Yun JY (2010) Indoor radon distribution of subway stations in a Korean major city. *J Environ Radioact.*, **101(4)**: 304-308.
18. Yafasov AY and Akimov VA (2001) Tectonic factor in the formation of the radon fields in the atmosphere of the Tashkent subway. *Atom Energy.*, **90(2)**: 130-136.
19. Deb A, Gazi M, Bhoumik G, Naskar A, Barman C (2017) Exposure to underground radon in and around Kolkata Municipal Corporation area: an exhaustive study. *J Radioanal Nucl Ch.*, **311**: 375-384.
20. Song MH, Chang BU, Kim YJ, Lee HY, Heo (2010) DH Radon in the underground workplaces; assessment of the annual effective dose due to inhaled radon for the Seoul subway station staffs. *J Radiat Protect Res.*, **35(4)**: 163-166.
21. Yilmaz Alan H, Akkus B, Amon Susam L (2019) Investigation of radon concentrations of underground metro and Marmaray stations in Istanbul. *J Radioanal Nucl Ch.*, **322**: 291-304.
22. The writing group of the summary report on nationwide survey of environmental radioactivity level in China (1992) Survey of concentrations of radon and α potential energy of Rn daughter products in air in some regions of China (1983-1990). *Radiat prot.*, **(02)**: 164-171.
23. CMA and SAC (2022) GB/T 18883-2022 Standards for indoor air quality, Beijing.
24. MEE (2021) HJ 1212-2021 Technical specifications for surface water environmental quality monitoring, Beijing.
25. AQSIQ and SAC (2015) GB/T 16146-2015 Requirements for control of indoor radon and its progeny, Beijing.
26. UNSCEAR (2000) Sources, effects and risks of ionizing radiation", Report to the general assembly with scientific annexes A and B. New York.
27. Loan TTH, Ba VN, Thien BN (2022) Natural radioactivity level in fly ash samples and radiological hazard at the landfill area of the coal-fired power plant complex, Vietnam. *Nucl Eng Technol.*, **54(4)**: 1431-1438.
28. Shi Y, Zhao J, Shi S, Ding B, Zhang J, Mohsen MA, Zhao H, Wei G, Zhang P, Jiang W, Wu P (2023) Radon concentration and radiation hazard of a rare earth waste dump in China. *Kuwait J Sci.*, **50(2)**: 148-152.
29. ICRP (1991) 1990 Recommendations of the international commission on radiological protection, ICRP Publication 60. Ann. ICRP 21(1-3).
30. ICRP (2007) The 2007 recommendations of the international commission on radiological protection, ICRP Publication 103. Ann. ICRP 37(2-4).
31. MOH (2002) GBZ 116-2002 Standard for controlling radon and its progenies in underground space, Beijing.
32. Colgan PA, Gutierrez J (1996) National approaches to controlling exposure to radon. *Environ Int.*, **22(1)**: 1083-1092.
33. AQSIQ (2002) GB 18871-2002 Basic standards for protection against ionizing radiation and for the safety of radiation sources, Beijing.
34. Taqi AH and Namq BF (2022) Radioactivity distribution in soil samples of the Baba Gurgur dome of Kirkuk oil field in Iraq. *Int J Envi-*

ron An Ch, 1-19.

35. Özden S and Akózcan S (2021) Natural radioactivity measurements and evaluation of radiological hazards in sediment of Aliağa Bay, Izmir (Turkey). *Arab J Geosci*, **14**: 64.

36. Weng X, Luo W, Wang Y, Jia Y, Wang S (2022) Atmospheric radon concentration in Guiyang Subway line 1 and the potential health effects. *Earth Env*, **50(1)**: 131-139.

37. Wang H, Shi M, Bai W, Shen Y, Liu H (2018) Analysis on radon concentration in Wuhan Subway. *J Pub Health Prev Med*, **29(2)**: 100-101.

38. Zhu X, Zhou C, Xu P (2012) Preliminary Investigation of Radon Radiological Level in Air of Nanjing Metro Station. *Adm Techn Envir Monit*, **24(1)**: 29-31.

39. Wang C (2015) Research on the distribution of radon concentrations in the air of Chengdu metro line 1 stations. *Sichuan Envir*, **34(1)**: 146-149.

40. Ci J, Shi J, Chen F, He W, Rao X, Li S, Li Z, Yang X (2006) Radiation levels and analysis of various station sections in the Phase 1 construction of the Shenzhen Metro. *Chin J Radiol Health*, **15(4)**: 474-475.

41. Liu X, Zhao X, Ma Y, Feng L, Lei J, Liang T, Xie P (2019) Study on the radon concentration and the surface level of γ radiation dose rate in the stations of Nanning metro line. *Chin J Radiol Health*, **28(1)**: 72-75.

42. Yu KN, Young ECM, Wong KC (1996) A survey of radon properties in underground railway stations in Hong Kong. *J Radiol Prot*, **16(1)**: 37.

43. Jing J, Lu X, Li C, Fu L, Shi L, Qiang L (2015) Investigations and analysis of radon concentration in Xi'an metro station. *Radiat Prot*, **35(5)**: 317-320.

44. Liendo J, Sajó-Bohus L, Pálfalvi J, Greaves ED, Gomez N (2017) Radon monitoring for health studies in the Caracas subway using SSNTDS. *Radiat Meas*, **28(1-6)**: 729-732.

45. Hwang SH and Park WM (2018) Radon and PM 10 concentrations in underground parking lots and subway stations with health risks in South Korea. *Environ Sci Pollut R*, **25**: 35242-35248.

46. Bassioni G, Labib MA, El-Faramawy N (2015) Unnoticed Daily Exposure to Radon in Cairo's Subway. *Egypt J Sci Res*, **133(4)**: 471-481.

47. Sundal AV, Henriksen H, Soldal O, Strand T (2004) The influence of geological factors on indoor radon concentrations in Norway. *Sci Total Environ*, **328(1-3)**: 41-53.

48. Moreno V, Baixeras C, Font L, Bach J (2008) Indoor radon levels and their dynamics in relation with the geological characteristics of La Garrotxa, Spain. *Radiat Meas*, **43(9-10)**: 1532-1540.

49. Hwang SH, Park JB, Park WM (2018) Radon and NO₂ levels and related environmental factors in 100 underground subway platforms over two-year period. *J Environ Radioactiv*, **181**: 102-108.

50. Bu-Olayan AH, Thomas BV (2016) Evaluation of radon pollution in underground parking lots by discomfort index. *Iran J Med Phys*, **13(2)**: 65-76.

51. Michèle V, Chahed N, Mtimet S (2004) Radon concentrations in some dwellings of Tunisia. *Health Phys*, **86(2)**: 150-154.

52. Schnell I, Potchter O, Yaakov Y, Epstein Y, Brener S, Hermesh H (2012) Urban daily life routines and human exposure to environmental discomfort. *Environ Monit Assess*, **184**: 4575-4590.

